Supplementary Materials

1. The FORECAST Model

1.1. Generation of Historical Rates of Ecological Processes

Stand growth and ecosystem dynamics estimations are based on the rates of the most important ecological processes involved in the availability of nutrients and light. The rates of these processes are calculated from a combination of historical bioassay data (biomass accumulation in component pools, stand density, *etc.*) and measured decomposition rates, photosynthetic saturation curves by relating biologically-active components (foliage and small roots) with calculations of nutrient uptake, light capture and net primary production (see [1] for a detailed description of the input parameters needed). With the calibration data obtained from different sources (see below), the model calculates the annual rates of different ecological processes (tree growth, litterfall production, mortality, nutrient mineralization from litter, *etc.*) based on the historical data on tree growth, understory growth and vegetation density provided by the user. For each plant species for which historical data are provided, the total net primary production (TNPP) that occurred for each annual time step (t, in years) is calculated with Equation (1).

$$TNPP_t = \Delta biomass_t + litterfall_t + mortality_t \tag{1}$$

where $\Delta biomass_t$ = the sum of the change in mass of all of the biomass components of the particular species in time step t; $litterfall_t$ = the sum of the mass of all ephemeral tissues that are lost in time step t (e.g., leaf, branch, bark and reproductive litterfall and root death); and $mortality_t$ = the mass of individual plants that die in time step t. The change in biomass ($\Delta biomass_t$) in each time step is derived from a series of age-biomass curves created with empirical data. Litterfall is calculated using user-defined values based on empirical litterfall rates. Mortality is derived from a series of age-stand density curves created with empirical data. Mortality is calibrated for each tree species through two different parameters: curves of historical stand density for different ages and the proportion of mortality that is due to non-interspecific competition factors. Together, both parameters allow simulating the endemic, low-level mortality events caused by pests and diseases typical of forests (for a detailed description on mortality simulation in FORECAST, see Kimmins, Mailly and Seely [2]).

The model also estimates the shade-corrected foliage N content (SCFN), which represents the amount of fully-illuminated foliar N that was required to produce the calculated historical TNPP. To estimate foliage shading, FORECAST simulates canopy foliage biomass as a "blanket" that covers the stand and that is divided into several layers of 0.25 m in height, each of them increasingly darker from the top to the bottom of the canopy. The light absorbed by each layer is calculated based on the foliage biomass present in each time step and a user-defined empirical curve of the foliage mass-proportion of full light (light absorption by foliage). Once an estimation of self-shading has been completed for a particular time step using the method described above, FORECAST calculates a foliar N content adjusted for the effects of self-shading (Equations (2) and (3)).

$$SCFN_t = \sum_{i=1}^{n}(FN_{t,i} \times PLSC_i) \tag{2}$$

$$FN_{t,i} = \text{foliage biomass}_{t,i} \times \text{foliar N concentration} \tag{3}$$

where $FN_{t,i}$ = the mass of foliage nitrogen in the *i*-th quarter-meter height increment in the live canopy at time *t*; $PLSC_i$ = the photosynthetic light saturation curve value for the associated light level in the *i*-th quarter-meter height increment in the live canopy; and n = the number of quarter-meter height increments in the live canopy at time *t*. The mean photosynthetic rate of the foliage in canopy level *i* is calculated by combining simulated light intensities in canopy level *i* with input data that define photosynthetic light saturation curves for the foliage type in question. Finally, the driving function curve for the potential growth of a given species in FORECAST is the shade-corrected foliar nitrogen efficiency (SCFNE) calculated for each annual time step (t) with Equation (4):

$$SCFNE_t = TNPP_t / SCFN_t$$

(4)

When data describing the growth of a species on more than one site quality (defined as the combination of nutrient availability and climate conditions for a specific site, see [3]) are provided, SCNFE function curves will be generated during the calibration stage for each site quality.

Net primary production in FORECAST is allocated among the different organs in the same ratios as the input data on biomass accumulation curves for each organ. If data are given for sites that differ in productivity, the model will simulate changing resource allocation strategies as the simulated nutritional site quality varies during a run of the model. Thus, empirically-observed variations in production allocation strategies on sites of different nutritional quality are used to guide the simulation of changing production allocation in response to simulated changes in nutritional site quality during the simulations.

Kimmins *et al.* [4] have shown how the combination of light and nutrient limitation is not enough to explain complex ecological patterns in models through models, and they recommended including understory vegetation also in the simulations. Therefore, a comparable, but simpler set of data for understory vegetation must be provided to represent this ecosystem component. Lastly, data describing decomposition rates for various litter and humus types are required to simulate nutrient cycling. Decomposition rates are defined by the user (using values from empirical studies) and are affected by site quality, which, in turn, is defined depending on nutrient and water availability [2]. Snags and logs are tracked by placing them into different categories depending on their original sizes (with slower decomposition rates for snags and for stems with larger sizes).

1.2. Model Initialization

To establish initial site conditions, we carried out a modified version of the typical spin-up process for initializing biogeochemical models, used to let the model reach a stable state [5,6], until it matches the observed site conditions of soil organic matter [7,8]. Initial conditions were created by running the model for 6, 9 or 18 consecutive 100-year cycles (for the poor, medium and rich sites, respectively; see below), ending with a stand-replacing windthrow to simulate natural disturbances by typhoons, the most common natural disturbance in Taiwan [9]. These runs were followed by a 50-year cycle without tree cover and with a woody crop harvested every year, to simulate the sugar cane management. These runs allowed the model to accumulate soil organic matter until reaching a stable value, which was used as the starting conditions for the scenarios.

1.3. Simulation of Tree and Plant Growth: Inter-Specific Competition in Mixed Stands

During the simulation stage, for each annual time step, the annual potential growth (APG) of each tree and understory species is driven by the photosynthetic production of the foliage biomass (Equation (5)). The productive capacity of a given quantity of foliage biomass (photosynthetic rate) is assumed to be dependent on foliage nitrogen content corrected for shading created by the canopy of the simulated site ($SCFN_t^*$). $SCFN_t^*$ is different from the $SCFN_t$ that was previously calculated during the internal calibration stage. During the simulation stage, the canopy simulated corresponds to the site defined by the user for that particular scenario, which can be different from the empirical canopy data used during the calibration stage, and therefore, $SCFN_t^*$ is particular for each simulation.

$$APG_{t+1} = SCFN_t^* \times SCFNE_t \tag{5}$$

where APG_{t+1} = the annual potential growth for a given species in the next time step. During the simulation stage, the model interpolates between the different curves of SCFNE calculated before to find the site quality of the simulated site.

Light competition among species is a function of the vertical distribution of the foliage of the different species, the foliage biomass in their canopies and the reduction in light per unit of foliage biomass. Then, a tall tree species with open canopy (low foliage biomass per hectare) will allow more light to pass to the understory than a shorter tree species with larger foliage biomass. Combined, the tall species will shadow the short species, and both trees will then shadow the understory. Nutrient uptake requirements to support APG are calculated based on rates of biomass growth and data on nutrient concentration in the different biomass components.

Nutrient dynamics in this study were restricted to nitrogen, a limiting nutrient in tropical and sub-tropical Taiwanese forests [10]. Carbon and nitrogen cycles are linked through the use of the foliar nitrogen efficiency as the driving function of the model (amount of biomass generated in a year per kg of foliar N). Therefore, a limitation in N uptake will result in a reduction of foliar N, reducing the biomass produced by the trees. Nutrient uptake demands on sites of different N fertility are based on observed biomass accumulation rates and tissue nutrient concentrations on these sites, allowing for internal cycling of nutrients.

After calculating how much of this demand can be met by internal retranslocation, the rest becomes the uptake demand for each species. The amount of soil nutrients available to a plant (tree or understory) species is a function of the total amount available in the soil, the degree to which the fine roots of the species occupy the soil (the ration between the current and maximum fine root biomass), and the competition for soil nutrients among the various species on the site. Where the total uptake demand of all plant species (trees and understory combined) exceeds the total available in the soil, competition will occur. The allocation between the species in such competitive situations will be in the ratio of their uptake demands, modified by their actual/maximum fine roots biomass ratios (a detailed description can be found in Kimmins [3]).

Nutrient availability is calculated based on empirical data describing litter and humus decomposition rates, changes in chemistry as decomposition proceeds and the size of nutrient pools in the mineral soil and humus (cation exchange capacity (CEC) and anion exchange capacity (AEC), respectively). If the availability of nutrients for each time step is less than required to support APG,

vegetation growth is limited by nutrients, and the realized annual growth is lower than APG. Nitrogen cycling in FORECAST is based on a mass balance approach, where N can exist in three distinct pools: (1) the plant biomass pool; (2) the available soil nutrient pool; and (3) the soil organic matter/forest floor pool. Inputs and outputs of N to the ecosystem are simulated in a four-stage process for each annual time step. The "available" N pool in FORECAST can be assimilated to represent the interchangeable N present in the soil during one year as NH_4^+, NO_3^- or labile organic N fractions with turnover rates shorter than one year. N deposition and N fixed by bryophytes and other microorganisms are simulated as constant annual N fluxes that directly reach the soil solution and are incorporated into the available N pool. The available N pool is calculated by simulating consecutively the different inputs and outputs of the biogeochemical cycle: deposition, fertilization, seepage, leaching, mineralization and immobilization. A detailed description of the simulation of each of these fluxes in FORECAST can be found in Kimmins *et al.* [2] and Blanco *et al.* [11]. The definition of site fertility based on N availability assumes that soil moisture is not limiting in these sites. FORECAST does not explicitly simulate soil moisture, and therefore, it does not uses weather data as model inputs. However, soil moisture is still implicitly affecting the simulation by the use of the parameter "maximum foliage per tree", which is directly correlated with soil moisture availability [2]. Given that the annual precipitation in the region is about 2000 mm, with peaks during summer, but with rainfall distributed along the whole year, the assumption to incorporate moisture in the simulations seems adequate.

Simulating of C and N in soil is achieved by assuming that SOM can be divided into two different pools: litter and humus. Litter is composed of a collection of different litter cohorts, each with its age and decomposition stage. Litter decomposition is defined by user-provided decomposition rates. When the decomposition process of each litter has ended (as defined by reaching a percentage of the initial mass), this material becomes part of the active humus. This pool represents resistant plant material derived from structural litter and soil-stabilized microbial products. Typical turnover rates for this pool range from 20 to 100 years, depending of the conditions simulated. The last SOM pool is the passive humus, which accumulates the remaining decomposed materials, represents material very resistant to decomposition and includes physically- and chemically-stabilized SOM, with typical turnover times between 200 to 2000 years. N content in these pools is defined by the N concentration in the senesced plant material and in the humus. Such an approach to SOM simulation is therefore similar to the one used in models, such as CENTURY [12], ROMUL [13] or ICBM [14].

2. Calibrating FORECAST for Mixed Subtropical Plantations in Eastern Taiwan

The model FORECAST was calibrated to simulate mixed plantation forests of the Taiwan Sugar Corporation in Hualien County (23.6°N, 121.4°E, elevation 100 m a.s.l., eastern Taiwan). The total afforestation area of the site is 1027 ha, and most of the trees were planted in 2002. According to the nearest weather station of the Central Weather Bureau (*ca*. 40 km to the north of the site), the 2004–2013 mean annual precipitation is 2230 mm and the mean annual air temperature is 24.4 °C. The seasonal variation of air temperature is typical for the subtropical region with a January mean of 18.6 °C and a July mean of 29.6 °C.

Data on historical tree growth patterns of camphor laurel were gathered from the literature [15–23] (Figures S1 and S2). Data on tree light and nitrogen requirements were derived from the literature [24–27]

(Tables S1 and S2). Decomposition rates were derived from the literature [19,28,29] (Table S4). For Himalayan ash, historical tree growth patterns were gathered from the literature [16,30–38]. Data on tree light and nitrogen requirements were derived from the literature [2–6,39–44]. Decomposition rates were derived from the literature [12,13,45–47]. The understory was simulated as grass and shrub complexes [48] (Table S3). Published data, modified to fit the observations in the research sites, were used to characterize shrub biomass, height, tissue nutrient concentrations and other relevant data [49–53].

Atmospheric deposition rates are assumed to equal areas with low levels of N deposition (5 kg ha^{-1} y^{-1} [54]). Soil is developed from fluvial material with a loamy sand or sandy loam texture. Due to the high content of pebbles (10%–40%), the soil depth is only 60–90 cm. Soil is classified to be Typic Dystrudepts following the USDS system. Information for the soil nutrient content of the site is still lacking (Table S4).
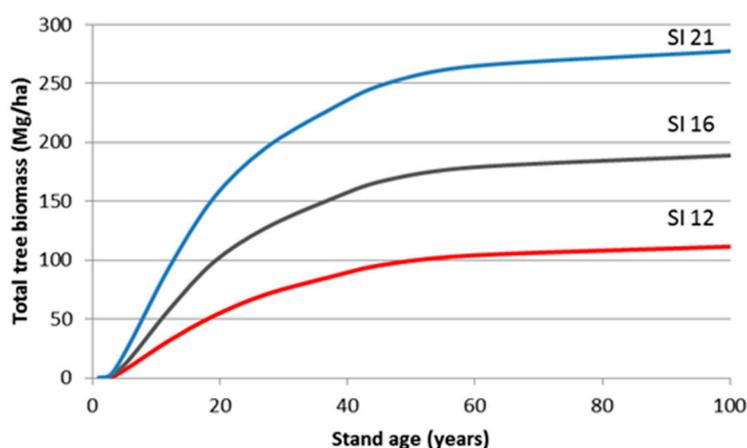
Figure S1. Total tree biomass curves used to calibrate camphor tree growth in FORECAST for three different site qualities (SI: site index, or top tree height at a stand age of 50 years). The three sites provide the pre-simulation calibration space for the model, and they do not represent the sites simulated in this research.
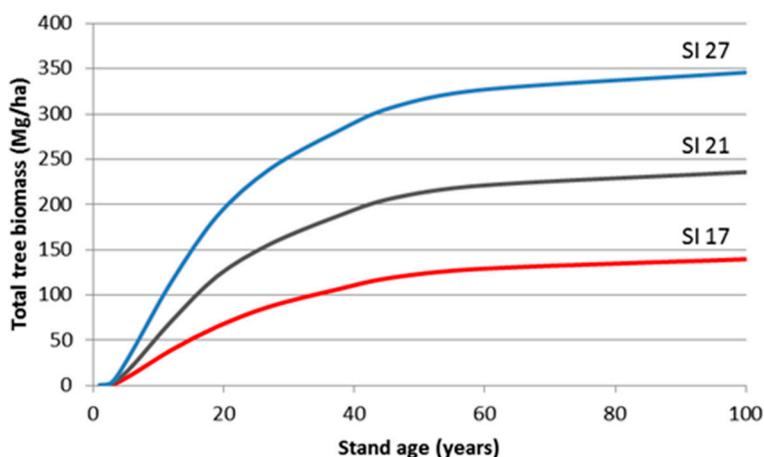
Figure S2. Total tree biomass curves used to calibrate Himalayan ash growth in FORECAST for three different site qualities (SI: site index, or top tree height at a stand age of 50 years). The three sites provide the pre-simulation calibration space for the model, and they do not represent the sites simulated in this research.

Table S1. Values used to calibrate FORECAST parameters related to camphor laurel.

Parameter	Unit	Poor site	Medium site	Rich site
Nitrogen concentration in leaves young/old/dead	%	1.25/0.79/0.67	1.35/0.90/0.69	1.45/0.92/0.69
Nitrogen concentration in stem sapwood/heartwood	%	0.16/0.03	0.16/0.03	0.18/0.04
Nitrogen concentration in bark live/dead	%	0.55/0.47	0.56/0.48	0.57/0.49
Nitrogen concentration in branches live/dead	%	0.47/0.27	0.57/0.28	0.67/0.29
Nitrogen concentration in root sapwood/heartwood	%	0.34/0.27	0.35/0.28	0.37/0.28
Nitrogen concentration in fine roots live/dead	%	0.81/0.56	0.91/0.56	1.06/0.56
Shading by maximum foliage biomass	% of full light	35	26	18
Soil volume occupied at maximum fine root biomass	%	100	98	95
Efficiency of N root capture	%	100	98	95
Retention time for young/old foliage/dead branches	y	1/0.50/35	1/0.50/35	1/0.50/30
Fine roots turnover	y^{-1}	1.40	1.15	0.90
Maximum foliage biomass/age of maximum foliage	kg tree^{-1}/y	6.0/25	10.0/22	25.0/20

Table S2. Values used to calibrate FORECAST parameters related to Himalayan ash.

Parameter	Unit	Poor site	Medium site	Rich site
Nitrogen concentration in leaves live/dead	%	1.40 /1.00	1.63 /1.07	1.80/1.17
Nitrogen concentration in stem sapwood/heartwood	%	0.20/0.04	0.22/0.04	0.24/0.04
Nitrogen concentration in bark live/dead	%	0.80/0.40	0.85/0.45	0.95/0.50
Nitrogen concentration in branches live/dead	%	0.60/0.22	0.63/0.26	0.65/0.30
Nitrogen concentration in root sapwood/heartwood	%	0.33/0.22	0.33/0.26	0.42/0.30
Nitrogen concentration in fine roots live/dead	%	0.90/0.70	1.07/0.77	1.18/0.77
Shading by maximum foliage biomass	% of full light	30	25	19
Soil volume occupied at maximum fine root biomass	%	100	98	95
Efficiency of N root capture	%	100	98	95
Retention time for young/old foliage/dead branches	y	1/0/35	1/0.50/35	1/0.50/30
Fine roots turnover	y^{-1}	1.20	1.00	0.90
Maximum foliage biomass/age of maximum foliage	kg tree^{-1}/y	7.0/25	10.0/22	13.0/20

Table S3. Values used to calibrate FORECAST parameters related to understory.

Grass complex parameters	Unit	Poor site	Medium site	Rich site
Nitrogen concentration in leaves live/dead	%	1.36/1.26	1.70/1.60	2.05/2.00
Nitrogen concentration in stems live/dead	%	1.10/0.20	1.37/0.25	1.65/0.30
Nitrogen concentration in rhizomes live/dead	%	1.25/1.00	1.56/1.25	1.87/1.50
Nitrogen concentration in roots live/dead	%	0.05/0.04	0.06/0.05	0.08/0.06
Shading by maximum foliage biomass	% of full light	0.20	0.15	0.05
Soil volume occupied at maximum fine root biomass	%	75	75	75
Efficiency of N root capture	%	99	99	99
Transfer from live to dead stem/rhizomes/roots	% y^{-1}	100/0/60	100/0/50	80/80/80
Retention time for foliage	y	1	1	1
Maximum foliage biomass/age of maximum biomass	Mg ha^{-1}/y	1.60/15	2.10/10	2.50/10
Shrub complex parameters				
Nitrogen concentration in leaves live/dead	%	1.12/1.02	1.40/1.30	1.68/1.68
Nitrogen concentration in stems live/dead	%	0.32/0.09	0.40/0.12	0.48/0.14
Nitrogen concentration in rhizomes live/dead	%	0.76/0.70	0.95/0.88	1.14/1.05
Nitrogen concentration in roots live/dead	%	0.07/0.05	0.09/0.07	0.11/0.08
Shading by maximum foliage biomass	% of full light	0.45	0.30	0.20
Soil volume occupied at maximum fine root biomass	%	75	75	65
Efficiency of N root capture	%	99	99	99
Transfer from live to dead stem/rhizomes/roots	% y^{-1}	20/20/40	20/20/30	20/20/30
Retention time for foliage	y	1	1	1
Maximum foliage biomass/age of maximum biomass	Mg ha^{-1}/y	1.80/50	2.20/40	2.80/35

Table S4. Values used to calibrate FORECAST parameters related to soil processes. Decomposition rates indicate the mass loss in one year as a fraction of the initial mass at that year.

Decomposition rates Camphor laurel		Litter age in years (Decomposition rate in %)		
Heartwood (by litter age)	% y^{-1}	1–10 years (0.4); 11–15 years (10.0); 16–25 years (15.0); 26–40 years (10.0); >40 years (2.0)		
Sapwood	% y^{-1}	1–5 years (2.0); 6–10 years (10.0); 11–15 years (30.0); 16–20 years (20.0); >20 years (4.0)		
Bark	% y^{-1}	1–5 years (2.0); 6–20 years (12.0); 21–40 years (20.0); >40 years (4.0)		
Large roots	% y^{-1}	1–2 years (8.0); 3–5 years (16.0); 6–15 years (30.0); 16–20 years (40.0); >20 years (4.0)		
Branches	% y^{-1}	1–5 years (10.0); 6–10 years (45.0); 11–15 years (35.0); >15 years (4.0)		
Leaves	% y^{-1}	1–2 years (70.0); 3–5 years (40.0); 6–7 years (35.0); >7 years (20.0)		
Fine roots	% y^{-1}	1 years (30.0); 2–3 years (50.0); >3 years (90.0)		
Himalayan ash				
Heartwood (by litter age)	% y^{-1}	1–3 years (0.8); 4–15 years (2.0); 16–25 years (12.0); 26–50 years (4.0); >50 years (1.0)		
Sapwood	% y^{-1}	1–3 years (0.8); 4–15 years (2.0); 16–25 years (12.0); 26–50 years (4.0); >50 years (1.0)		
Bark	% y^{-1}	1–10 years (5.0); 11–20 years (30.0); >20 years (10.0)		
Large roots	% y^{-1}	1–2 years (8.0); 3–5 years (16.0); 6–15 years (30.0); 16–20 years (40.0); >20 years (4.0)		
Branches	% y^{-1}	1–4 years (3.0); 5–11 years (15.0); 12–20 years (10.0); 21–35 years (5.0); >35 years (1.0)		
Leaves	% y^{-1}	1–5 years (43.0); 6–7 years (35.0); >7 years (20.0)		
Fine roots	% y^{-1}	1 years (30.0); 2–3 years (50.0); >3 years (90.0)		
Soil parameters		Poor site	Medium site	Rich site
Nitrogen concentration in slow/fast humus	%	3.00/1.40	3.00/1.40	3.00/1.40
Decomposition rate slow/fast humus	% y^{-1}	0.15/2.00	0.15/2.00	0.15/2.00
CEC soil (CEC humus)/AEC [*]	kg N ha^{-1}	40.0 (0.2)/5.0	60.0 (0.2)/10.0	80.0 (0.2)/20.0
Atmospheric deposition/seepage	kg N ha^{-1} y^{-1}	4.90/0.50	4.90/1.50	4.90/2.50
Non-symbiotic N fixation rate	Kg N ha^{-1} y^{-1}	1.0	1.0	1.0

[*] CEC: Cation Exchange Capacity; AEC: Anion Exchange Capacity.

References

1. Landsberg, J. Modelling forest ecosystems: State of the art, challenges, and future directions. *Can. J. For. Res.* **2003**, *33*, 385–397.
2. Kimmins, J.P.; Mailly, D.; Seely, B. Modelling forest ecosystem net primary production: The hybrid simulation approach used in FORECAST. *Ecol. Model* **1999**, *122*, 195–224.
3. Kimmins, J.P. *Scientific Foundations for the Simulation of Ecosystem Function and Management in FORCYTE-11*; Information Report NOR-X-328: 1993; Forestry Canada, Edmonton, AB, Canada; p. 88.
4. Kimmins, J.P.; Blanco, J.A.; Seely, B.; Welham, C.; Scoullar, K. Complexity in modelling forest ecosystems: How much is enough? *For. Ecol. Manag.* **2008**, *256*, 1646–1658.
5. Hashimoto, S.; Wattenbach, M.; Smith, P. A new scheme for initializing process-based ecosystem models by scaling soil carbon pools. *Ecol. Model.* **2011**, *222*, 3598–3602.
6. Shi, M.; Yang, Z.-L.; Lawrence, D.M.; Dickinson, R.E.; Subin, Z.M. Spin-up processes in the Community Land Model version 4 with explicit carbon and nitrogen components. *Ecol. Model.* **2013**, *263*, 308–325.
7. Blanco, J.A.; Seely, B.; Welham, C.; Kimmins, J.P.; Seebacher, T.M. Testing the performance of a forest ecosystem model (FORECAST) against 29 years of field data in a *Pseudotsuga menziesii* plantation. *Can. J. For. Res.* **2007**, *37*, 1808–1820.
8. Seely, B.; Welham, C.; Kimmins, J.P. Carbon sequestration in a boreal forest ecosystem: results from the ecosystem simulation model, FORECAST. *For. Ecol. Manag.* **2002**, *169*, 123–135.
9. Xi, W.; Chen, S.-H.V.; Chu, Y.-C. The synergistic effects of typhoon and earthquake disturbances on forest ecosystems: lessons from Taiwan for ecological restoration and sustainable management. *Tree For. Sci. Biotechnol.* **2012**, *6*, 27–33.
10. Owen, J.S. Stable nitrogen isotopes in a forested watershed in Taiwan. *J. For. Sci.* **2013**, *29*, 116–124.
11. Blanco, J.A.; Wei, X.; Jiang, H.; Jie, C.-Y.; Xin, Z.-H. Impacts of enhanced nitrogen deposition and soil acidification on biomass production and nitrogen leaching in Chinese fir plantations. *Can. J. For. Res.* **2012**, *42*, 437–450.
12. Parton, W.J.; Schimel, D.S.; Cole, C.V.; Ojima, D.S. Analysis of factors controlling soil organic matter levels in Great Plains grasslands. *Soil Sci. Soc. Am. J.* **1987**, *51*, 1173–1179.
13. Chertov, O.G.; Komarov, A.S.; Nadporozhskaya, M.; Bykhovets, S.S.; Zudin, S.L. ROMUL—A model of forest soil organic matter dynamics as a substantial tool for forest ecosystem modeling. *Ecol. Model* **2001**, *138*, 289–308.
14. Andrén, O.; Kätterer, T. Basic principles for soil carbon sequestration and calculating dynamic country-level balances including future scenarios. In *Assessment Methods for Soil Carbon*; Lal, R., Kimble, J.M., Follett, R.M., Stewart, B.A., Eds.; Lewis Publishers: Boca Ratón, FL, USA, 2001; pp. 495–511.
15. Wu, G. Effect of acidic deposition on productivity of forest ecosystem and estimation of its economic losses in southern suburbs of Chongqing, China. *J. Environ. Sci. (China)* **1998**, *10*, 210–215.
16. Hsui, Y.R.; Horng, F.W.; Chen, Y.H.; Chang, N.H. Planting performance of natural hardwood species on a degraded site in the Liukuei area. *Taiwan J. For. Sci.* **2001**, *16*, 115–124. (In Chinese)

17. Lei, P.F.; Xiang, W.H.; Tian, D.L.; Fang, X. Carbon storage and distribution in *Cinnamomum camphor* plantation. *Chin. J. Ecol.* **2004**, *23*, 25–30. (In Chinese)

18. Xiao, Y.; Liu, S.; Wang, G.J. Carbon storage of 4 forest ecosystem in Hunan Province. *J. Nat. Sci. Hunan Norm. Univ.* **2010**, *33*, 124–128.

19. Li, Z.H.; Nie, K.Y. Growth conditions and productivity of *Cinnamomum camphora* in karst areas of western Hunan. *J. Cent. South Univ. For. Technol.* **2011**, *31*, 12–16, 20.

20. Li, S.Z.; Tian, D.L.; Wang, G.J.; Yan, W.D.; Zhu, F. Time-space dynamics of fine root biomass in *Cinnamomum camphora* plantations in Changsha, Hunan. *J. Cent. South Univ. For. Technol.* **2008**, *28*, 51–55. (In Chinese)

21. Li, J.B.; Yan, W.D.; Ma, X.H. Litterfall production and nutrient dynamics of C*innamomum camphora* in subtropical region. *J. Cent. South Univ. For. Technol.* **2011**, *31*, 223–228. (In Chinese).

22. Tian, X.Q.; Wei, X.L. Effect of different ecological environments on plantation growth of *Cinnamomum bodineri* in Guizhou. *Guizou Agric. Sci.* **2011**, *39*, 184–187.

23. Yu, K.S. The Tree Plantations in the Lin-Kuo Area. Master's Thesis, National Taiwan University, Taipei, Taiwan, 2001.

24. Kuo, L.S. Effect of Growth Seasons on the Leaf Element Concentration of Four Street Tree Species in Taipei. Master's Thesis, National Taiwan University, Taipei, Taiwan, 2002.

25. Hong, L.W.; Wang, Y.N. Net photosynthetic productivity at different canopy layers of *Cinnamomum camphora. Q. J. Chin. For.* **2003**, *36*, 27–38 (In Chinese).

26. Kimmins, J.P. *Forest Ecology: A Foundation for Sustainable Forest Management and Environmental Ethics in Forestry*, 3rd ed.; Pearson Prentice Hall: Upper Saddle River, NJ, USA, 2004.

27. Chung, H.Y.; Liu, C.P. Effects of different densities on the growth and physiological responses of *Cinnamomum camphora* seedlings. *Q. J. Chin. For.* **2010**, *43*, 543–555. (In Chinese).

28. He, X.B.; Lin, Y.H.; Han, G.M.; Ma, T.W. Litterfall interception by understorey vegetation delayed litter decomposition in Cinnamomum camphora plantation forest. *Plant Soil* **2013**, *372*, 207–219.

29. Agren, G.I.; Bosatta, E. *Theoretical Ecosystem Ecology: Understanding Element Cycles*; Cambridge University Press: Cambridge, UK, 1996.

30. Chou, P.Y. The Seedling Growth and Photosynthetic Characteristics of Three Taiwan Native Hardwood Species Seedlings Acclimated under Different Light Environments. Master's Thesis, National Taiwan University, Taipei, Taiwan, 2004.

31. Lin, G.S. *Effect of Thinning Intensity on Volume Stock and Aboveground Biomass in a Farm Afforestation*; Forestry Bureau of Taiwan: Taipei, Taiwan, 2008; p. 62. (In Chinese).

32. Huang, Y.H.; Chung, C.H.; Chiu, C.M.; Lin, C.J. Tree ring characteristics of 7-year-old *Zelkova serrata*, *Melia azedarach*, and *Fraxinus formosana* in plains. *Q. J. Chin. For.* **2010**, *43*, 201–212. (In Chinese)

33. Chiang, P.N.; Wang, Y.N.; Leong, C.M. Study on growth and carbon storage of *Fraxinus griffithii* plantation in Central Taiwan. *J. Exp. For. Natl. Taiwan Univ.* **2010**, *24*, 185–194. (In Chinese)

34. Lin, C.S.; Ma, S.E. A simulation of the stand dynamic of *Fraxinus formosana* forest in cultivated land using the SORTIE-ND model. *J. Exp. For. Natl. Taiwan Univ.* **2010**, *23*, 63–78. (In Chinese)

35. Lin, Y.P. Crown Characteristics and Carbon Storage of *Zelkova serrata* and *Fraxinus formosana* of Afforesttation in Yunlin district. Master's Thesis, National Chung Hsing University, Taichung, China, 2011.

36. Lin, K.C.; Duh, C.T.; Huang, C.M. Estimate of carbon storage and sequestration of *Fraxinus griffithii* plantations in Taiwan. *Q. J. Chin. For.* **2010**, *43*, 261–276. (In Chinese)

37. Yang, M.X. Individual Tree Mortality Models for Six Plantations in Taiwan. Master's Thesis, National ILan University, ILan, Taiwan, 2011.

38. Liao, Y.W.; Chen, M.K.; Chen, Y.K.; Chung, Y.L.; Wu, S.T. Use SPOT satellite images to estimate the afforestation carbon storage of Taiwan Sugar Corporation in Ping-Tung. *J. Photogramm. Remote Sens.* **2011**, *16*, 101–113. (In Chinese)

39. Kuo, Y.L.; Fan, K.S.; Hwang, C.W.; Lee, Y.P.; Wu, H.L.; Tsay, R.F. Gas exchange potential in sun-exposed leaves of 30 broadleaf tree species in Taiwan. *Taiwan J. For. Sci.* **2004**, *19*, 375–386. (In Chinese)

40. Kazda, M.; Salzer, J.; Reiter, I. Photosynthetic capacity in relation to nitrogen in the canopy of a *Quercus robur*, *Fraxinus angustifolia* and *Tilia cordata* flood plain forest. *Tree Physiol.* **2000**, *20*, 1029–1037.

41. Penn, C.J.; Will, R.; Fultz, L.; Hamilton, D. Forage and tree seedling growth in a soil with an encased swine sludge layer. *J. Environ. Manag.* **2013**, *128*, 586–593.

42. Jia, S.X.; Wang, Z.Q.; Li, X.P.; Zhang, X.P.; Mclaughlin, N.B. Effect of nitrogen fertilizer, root branch order and temperature on respiration and tissue N concentration of fine roots in *Larix gmelinii* and *Fraxinus mandshurica*. *Tree Physiol.* **2011**, *31*, 718–726.

43. Fan, P.P.; Jiang, Y.X. Nitrogen dynamics differed among the first six root branch orders of *Fraxinus mandshurica* and *Larix gmelinii* during short-term decomposition. *J. Plant Res.* **2010**, *123*, 433–438.

44. Hölscher, D. Leaf traits and photosynthetic parameters of saplings and adult trees of co-existing species in a temperate broad-leaved forest. *Basic Appl. Ecol.* **2004**, *5*, 163–172.

45. Castro-Díez, P.; González-Muñoz, N.; Alonso, A.; Gallardo, A.; Poorter, L. Effects of exotic invasive trees on nitrogen cycling: a case study in Central Spain. *Biol. Invasions* **2009**, *11*, 1973–1986.

46. Jacob, M.; Viedenz, K.; Polle, A.; Thomas, F.M. Leaf litter decomposition in temperate deciduous forest stands with a decreasing fraction of beech (*Fagus sylvatica*). *Oecologia* **2010**, *164*, 1083–1094.

47. Vesterdal, L.; Elberling, B.; Christiansen, J.R.; Callesen, I.; Schmidt, I.K. Soil respiration and rates of soil carbon turnover differ among six common European tree species. *For. Ecol. Manag.* **2012**, *264*, 185–196.

48. Bi, J.; Blanco, J.A.; Seely, B.; Kimmins, J.P.; Ding, Y.; Welham, C. Yield decline in Chinese-fir plantations: a simulation investigation with implications for model complexity. *Can. J. For. Res.* **2007**, *37*, 1615–1630.

49. Xin, Z.H.; Jiang, H.; Jie, C.Y.; Wei, X.H.; Blanco, J.; Zhou, G.M. Simulated nitrogen dynamics for a *Cunninghamia lanceolata* plantation with selected rotation ages. *J. Zhejiang Agric. For. Univ.* **2011**, *28*, 855–862.

50. Fan, S.H.; Ma, X.Q.; Fu, L.S.; Liu, A.Q. Comparative study on underground vegetation development of different generation plantations of Chinese-fir. *For. Res.* **2001**, *14*, 8–16. (In Chinese)

51. Lin, K.M.; Yu, X.T.; Hong, W.; Huang, B.L. Effects of undergrowth plant on soil fertility in Chinese fir plantation. *Scientia Silvae Sinicae* **2001**, *37*, 94–98.

52. Xiang, W.H.; Tian, D.L.; Yan, W.D.; Kang, W.X.; Fang, X. Biomass dynamic and nutrient accumulation of natural restoration at early stage after fallow in clear-cutting forestland of Chinese fir plantation. *Acta Ecologica Sinica* **2003**, *23*, 695–702.

53. Yan, W.D.; Tian, D.L.; Jiao, X.M. A study on biomass dynamics and distribution of undervegetation in the secondary generation of Chinese-fir plantation in Hui Tong. *For. Res.* **2003**, *16*, 323–327.

54. Wei, X.H.; Blanco, J.A.; Jiang, H.; Kimmins, J.P. Effects of nitrogen deposition on carbon sequestration in Chinese fir forest ecosystems. *Sci. Total Environ.* **2012**, *416*, 351–361.